

UC Berkeley
SEMM Reports Series

Title

Some wave propagation problems in plastic-viscoplastic materials

Permalink

<https://escholarship.org/uc/item/3pn47205>

Authors

Lubliner, Jacob

Valathur, Munirathnam

Publication Date

1968-09-01

REPORT NO. 68-10

STRUCTURES AND MATERIALS RESEARCH
DEPARTMENT OF CIVIL ENGINEERING

SOME WAVE PROPAGATION PROBLEMS IN PLASTIC-VISCOPLASTIC MATERIALS

J. LUBLINER
and
M. VALATHUR

Interim Technical Report
U.S. Army Research Office (Durham)
Project No. 4547-E

SEPTEMBER, 1968

STRUCTURAL ENGINEERING LABORATORY
UNIVERSITY OF CALIFORNIA
BERKELEY CALIFORNIA

Structures and Materials Research
Department of Civil Engineering
Division of Structural Engineering
and Structural Mechanics

Report Number 68-10

SOME WAVE PROPAGATION PROBLEMS IN
PLASTIC-VISCOPLASTIC MATERIALS

by

J. Lubliner
Associate Professor of Civil Engineering
University of California, Berkeley

and

M. Valathur
Research Assistant
University of California, Berkeley

Contract Number DA-31-124-ARO-D-460
DA Project No: 20014501B33G
ARO Project No: 4547-E

Interim Technical Report
U. S. Army Research Office (Durham)
Project No: 4547-E

Structural Engineering Laboratory
University of California
Berkeley, California
September, 1968

CONTENTS

	PAGE
1. INTRODUCTION	1
2. EXAMINATION AND ASSUMPTIONS OF CONSTITUTIVE EQUATION	4
3. THE IMPACT PROBLEM	9
4. WAVE-PROPAGATION IN A FINITE BAR	14
5. EFFECT OF ABSORPTION DISTANCE	16
6. COMPUTATIONAL PROCEDURE	18
7. GENERAL SOLUTION	20
8. NUMERICAL EXAMPLES	24
9. CONCLUSIONS	27
REFERENCES	29
LIST OF FIGURES	32

SOME WAVE PROPAGATION PROBLEMS IN
PLASTIC-VISCOPLASTIC MATERIALS

1. Introduction:

Virtually all problems involving wave propagation in metals are analysed on the basis of one of two hypotheses: (1) the rate-independent" hypothesis proposed independently by Karman [30], Taylor [28] and Rakhmatulin [24], according to which the stress-strain curve of the material is independent of the rate of deformation or loading, as in the usual theory of plasticity; and (2) the "rate-dependent" hypothesis due to Sokolovsky [27] and Malvern [21], according to which the material is viscoplastic.

It was shown later by Simmons, Hauser and Dorn [26] that a uniaxial constitutive equation of the form

$$\dot{\epsilon} = f(\sigma, \epsilon)\sigma + g(\sigma, \epsilon) \quad (1.1)$$

includes as special cases, both of the above hypotheses, the first corresponding to $g(\sigma, \epsilon) \equiv 0$, and the second to $f(\sigma, \epsilon) = E^{-1}$ (E being the elastic modulus) with $g(\sigma, \epsilon) = 0$ being the equation of the static stress-strain curve. Similar results were obtained independently by Cristescu [9] and Lubliner [19].

In accordance with nomenclature proposed recently by Cristescu [9], a material described by a constitutive equation (1.1) will be referred to as "plastic-viscoplastic" with "plastic" and "viscoplastic" referring to the respective special types. (It is implied that such materials also possess an elastic range, so that terms such as "elastic-plastic-viscoplastic" may be dispensed with.)

Since most experimental studies have shown that real materials do not behave exactly according to either hypothesis (while the discrepancies have

generally been attributed by the proponents of both approaches to the effects of lateral inertia, the recent results of Baker and Yew [3] using torsional impact, are open to no such interpretation), Lubliner [19] suggested that the more general constitutive equation (1.1) be used in the numerical solution of wave-propagation problems, and that the results approximating those of either hypothesis may be obtained in extreme cases. He further showed [20] on the basis of an extremely simple, piece-wise linear, model of plastic-viscoplastic behavior, that results approaching the viscoplastic hypothesis will be obtained under one or more of the following circumstances: (1) weak impact, (2) long bar, (3) short "relaxation" time (or natural time of the material); that converse conditions will lead to results approaching the plastic hypothesis; and that intermediate conditions require the use of the general constitutive equation.

The purpose of the present study is to test further the validity of Lubliner's suggestions by means of numerical solutions of representative wave-propagation problems in bars whose mechanical behavior is described by equation (1.1) (slightly modified to account for loading-unloading behavior) with the functions $f(\sigma, \epsilon)$ and $g(\sigma, \epsilon)$ so chosen as to fit the observed behavior of some actual materials.

The chief benefit of equation (1.1) is that it accounts for the existence of distinct static and dynamic plastic stress-strain relations, the former being given by $g(\sigma, \epsilon) = 0$ and the latter by a solution of the differential equation

$$\frac{d\epsilon}{d\sigma} = f(\sigma, \epsilon)$$

subject to the initial condition $\sigma = 0$ when $\epsilon = 0$. Theoretically, then, a "dynamic" stress-strain curve corresponds to infinite rates of strain and stress. Practically, the strain rates attained in impact tests on bars are

of the order of $10^2 - 10^3 \text{ sec.}^{-1}$ (strain rates of order 10^4 sec.^{-1} have been obtained only by using the split Hopkinson bar, and the simplifying assumptions used in analysing the results must be corrected.)* Materials whose stress-strain curves are still rate-sensitive at these rates (e.g. mild steel, annealed pure aluminum [13, 17]) may therefore be treated on the basis of viscoplastic behavior, that is, we may set $f(\sigma, \epsilon) = E^{-1}$, with the knowledge that this may need to be modified if higher strain rates become practicable. On the other hand, some materials (e.g. age-hardened aluminum alloys) show almost no rate sensitivity at these strain rates, at least at room temperature, so that we may set $g(\sigma, \epsilon) = 0$.

A direct measurement of the effect of changing the strain rate during a compression test at room temperature was performed by Holt et al. [13] on a series of commercial alloys in both the o and T6 tempers. From their test results, it can be seen that even at the comparatively small strain-rate change, the assumption of strain-rate independence holds only for age-hardened alloys, as pointed out previously. Further it can be seen that the stress-strain curves, for higher strain-rates of 10^2 sec.^{-1} to 10^3 sec.^{-1} , all coincide. This means that for understanding the behavior of that particular material under high strain-rate deformation, the existence of dynamic stress-strain curve can be assumed.

The purpose of this study is not a comparison of results obtained by applying the present theory with experimental data, but rather the derivation of a quantitative criterion for determining when strain-rate effects become significant, since it has been shown qualitatively [19] that under given circumstances either the "viscoplastic" theory due to Sokolovsky [27] and Malvern [21] or the older, "rate-independent" theory of Karman [30], Taylor [28] and Rakhmatulin [24], may provide a valid approximation.

* J. Klepaczko, private communication.

2. Examination and Assumptions of Constitutive Equation:

The constitutive equation (1.1) must now be examined in the light of its implications. This will entail a modification of its form which will reasonably well represent the physical situation observed experimentally by various authors in their investigations [11,13,15,17], before one can proceed to a formulation of the wave propagation problem. (In the ensuing discussion, positive changes in stress will represent loading, whether compressive or tensile; the direction of the velocity must be defined accordingly.) (i)

The equation

$$g(\sigma, \varepsilon) = 0 \quad (2.1)$$

describes the static stress-strain relation, which may be written in an explicit form, for example as a stress-strain equation

$$\sigma = h(\varepsilon) \quad (2.2)$$

or as a strain-hardening equation

$$\sigma = \sigma_s + \phi_s(\varepsilon_p), \quad \varepsilon_p > 0 \quad (2.3)$$

where $\varepsilon_p = \varepsilon - \frac{\sigma}{E}$ is the plastic deformation ($E = \text{Young's modulus}$), σ_s is the static elastic limit and $\phi_s(\varepsilon_p)$ is the static strain-hardening function, having the properties

$$\begin{aligned} \phi_s(0) &= 0 \\ \phi_s'(\varepsilon_p) &\geq 0, \quad \varepsilon_p > 0 \end{aligned} \quad (2.4a)$$

also if the metal has no sharp yield point;

$$\phi_s'(0) = \infty \quad (2.4b)$$

It should be remarked that a static strain-hardening law exists only at lower temperatures, at which there is no steady-state creep. (ii) Under a constant load, i.e., $\dot{\sigma} = 0$, we have

$$\dot{\epsilon} = g(\sigma, \epsilon) \quad (2.5)$$

describing in general, transient creep without thermal recovery, though the creep becomes steady if $\partial g / \partial \epsilon$ vanishes. Clearly, transient creep cannot take place when the stress is below the static yield level, hence the function $g(\sigma, \epsilon)$ must have the same sign as $\{\sigma - h(\epsilon)\}$ and must be replaced in (1.1) by $\langle g(\sigma, \epsilon) \rangle$, where

$$\langle Z \rangle \equiv \begin{cases} Z, & Z > 0 \\ 0, & Z < 0. \end{cases}$$

(iii) When the stress and strain rates are very high (theoretically infinite), we have dynamic loading, governed by the differential equation

$$\frac{d\epsilon}{d\sigma} = f(\sigma, \epsilon) \quad (2.6)$$

The integral curves of (2.6) are dynamic loading curves corresponding to different initial states characterized by one parameter, for example the initial plastic deformation ϵ_{p_0} . The general solution of (2.6) may thus be written in the form

$$\sigma = h_d(\epsilon, \epsilon_{p_0}) \quad (2.7)$$

If such curves are found experimentally, as in [32], then the value of $f(\sigma, \epsilon)$ is simply the inverse slope of the curve passing through (σ, ϵ) .

(iv) The discussion in the preceding subsection applies to loading, i.e., $\dot{\sigma} > 0$. In an elastic-plastic material unloading takes place elastically. Consequently, the complete constitutive equation, replacing (1.1) is

$$\dot{\epsilon} = \langle g(\sigma, \epsilon) \rangle + \begin{cases} f(\sigma, \epsilon) \dot{\sigma} & \dot{\sigma} > 0 \\ \frac{1}{E} \dot{\sigma} & \dot{\sigma} < 0 \end{cases} \quad (2.8)$$

Further, the static stress-strain equation $\sigma = h(\epsilon)$ is interpreted as a succession of equilibrium states such that flow occurs only when the flow condition

$$\sigma > h(\epsilon)$$

is satisfied; otherwise the elastic law applies.

The use of this flow condition implies that if the strain-rate during the test is finally reduced to zero so that a state of equilibrium under load is reached, the equilibrium point will lie on the static stress-strain curve.* Hence when the strain-rate is very very low (theoretically zero), we have static loading.

Based on the assumption that the value of strain-rate equal to $10^{-3} \text{ sec.}^{-1}$ is sufficiently low, we can assume the $\sigma - \epsilon$ curve for $\dot{\epsilon} = 10^{-3} \text{ sec.}^{-1}$ to be the static loading curve in our further discussions.

Also, since the maximum strain-rates attained in impact tests on bars are of the order of $10^2 - 10^3 \text{ sec.}^{-1}$, we can assume that this value of strain-rate is theoretically infinite for the practical purposes of plastic wave-propagation studies, and hence we can consider the $\sigma - \epsilon$ curve corresponding to such a value of strain-rate, to be the "dynamic loading curve". Following the discussion of subsection 2-(iii), i.e., the equation (2.7) with zero initial plastic deformation, the function $\sigma = h_d(\epsilon)$ is simply the experimentally obtained $\sigma - \epsilon$ curve for maximum strain-rate; to be referred to hereafter as the dynamic loading curve.

Since the Ramberg-Osgood equation for describing stress-strain curves [17] has been found to apply for a number of structural materials, the same

* This neglects strain-rate history.

equation will be used here also, to describe the dynamic loading curve. It has the form

$$\epsilon = \frac{\sigma}{E} + K \sigma^n \quad (2.9)$$

ϵ = conventional total strain (in/in)

σ = applied stress (ksi)

E = elastic modulus (ksi)

K = material parameter

n = material parameter (shape factor)

The modulus E is taken directly from stress-strain curves, whereas K and n are calculated by the method of offsets. The geometric slope of a logarithmically plotted plastic strain versus stress curve gives n . K is calculated by rearrangement of the plastic deformation term ($K \sigma^n$) of equation (2.9):

$$K = \epsilon_p / \sigma^n \quad (2.10)$$

where ϵ_p = plastic deformation (in/in).

Hence equation (2.9) represents the (assumed) dynamic loading curve.

Differentiation of equation (2.9) yields

$$\frac{d\epsilon}{d\sigma} = \left[\frac{1}{E} + Kn \sigma^{n-1} \right] \quad (2.11)$$

Hence from equations (2.6) and (2.11) we have

$$f(\sigma, \epsilon) = \frac{1}{E} + Kn \sigma^{n-1} \quad (2.12)$$

On the other hand, from the basic concepts of irreversible thermodynamics, we know that the total strain-rate can be separated into reversible and irreversible parts. The irreversible strain rate is a function of stress,

strain and temperature, i.e.,

$$\underline{D}^i = \psi(\underline{\sigma}, \underline{\varepsilon}^i, T) \quad (2.13)$$

where the superscript 'i' refers to the irreversible part; T is the temperature. In the case of uniaxial stress,

$$\dot{\varepsilon}^i = \psi(\sigma, \varepsilon^i, T) \quad (2.14)$$

As for $\psi(\sigma, \varepsilon^i, T)$, though many forms have been assumed, in particular,

$$\dot{\varepsilon}^i = A_1 (\varepsilon^i)^{-\alpha} \exp(\beta\sigma) \quad (2.15a)$$

is employed most frequently in the literature. Consequently, to account for the high flow stress, the form

$$\dot{\varepsilon}^i = A_2 (\varepsilon^i)^{-\alpha} \sinh(\beta\sigma) \quad (2.15b)$$

may be assumed as an appropriate one. It is assumed that A_2 , α and β depend on temperature also.

Further examination of equation (2.15b) reveals that as a consequence of the results of subsection 2-(ii), an admissible form of $g(\sigma, \varepsilon)$ for the high flow stress and room temperature, is

$$g(\sigma, \varepsilon) = A(\varepsilon + C)^{-2} \sinh\left\{\frac{\sigma - h(\varepsilon)}{B}\right\} \quad (2.16)$$

where A, C and B are constants to be determined empirically from test data.

It is to be noted that, in order to determine the constants A, C and B in equation (2.16), we need data for at least one intermediate strain rate, besides the (assumed) static and dynamic loading curves.

3. The Impact Problem:

The distinguishing feature of impulsive loading arises from the fact that the action of a suddenly applied load is not simultaneously transmitted to all parts of the body, parts of the body remote from the point of application of the load remain undisturbed until the localized stresses in reaction to the load are propagated to those parts; the finite velocity of propagation of such "waves" depends upon inertial effects and upon the mechanical behavior of the material comprising the body. In this section, the governing differential equations appropriate for stress-wave propagation based on a minimal assumption sufficient for the mathematical establishment of wave propagation, will be developed.

The equations governing the propagation of stress waves can be developed by means of either the Eulerian or the Lagrangian co-ordinate system. But Lagrangian co-ordinates exhibit one significant advantage over Eulerian co-ordinates, in that they provide a very simple expression for the law of conservation of mass. In order to take the advantage of this simplicity, Lagrangian co-ordinates will be adopted throughout the following discussion.

As a result of the substantial difficulties that are encountered, no satisfactory description of plastic deformation in three dimensions has yet been formulated. For that reason, it will be necessary to limit the present discussion to the simple linear case of waves moving along the axis of a uniform rod. Also it must be remembered that the deformation of rods under a longitudinal impact is three-dimensional in nature. Obviously much additional theoretical development will be necessary before the theory can be applied with confidence to practical problems of impact forming of metals where three-dimensional analyses will be required and where unruly boundary conditions are encountered.

It is well known, for the purely elastic case, that the results obtained by the approximation of uniaxial stress are fairly accurate only when the rate of change of stress and strain are small. One would expect that the same argument would hold to some degree when plastic deformation is allowed. However, in most experiments concerned with longitudinal elastic-plastic pulse propagation along bars, the end condition is either a normal velocity or a normal stress whose time dependence is that of a step function. This indicates that the effect of lateral inertia could be considerable. The one-dimensional approximate equations are modified in references [10] and [15] to include the effect of lateral inertia. These equations are then modified in references [10] to allow for plastic deformation and hysteresis in addition to the lateral inertia effect. It was concluded [10] that some observations set forth as proof of the existence of a strain-rate effect might equally be explained, at least qualitatively, on the basis of lateral inertia effects.

A torsional impact, wherein no radial motion of the specimen is produced, eliminates in the most direct manner the dimensional discrepancy between the mathematical model and experimental investigation which exists in longitudinal impact studies.

To formulate the impact problem for an initially uniform bar, whose behavior is given by the constitutive equation (1.1), we must adduce the equations of motion and of continuity, and specify initial and boundary conditions. Since the Lagrangian co-ordinate system is more convenient, the "engineering" definition of stress and strain will be used; furthermore, these will be counted as positive in compression. If x denotes the initial distance of a section of the bar from the left end and v its velocity, we have

$$\frac{\partial \sigma}{\partial x} = - \rho \frac{\partial v}{\partial t} \quad (3.1)$$

and

$$\frac{\partial \varepsilon}{\partial t} = - \frac{\partial v}{\partial x} \quad (3.2)$$

where σ , ε , ρ , t denote stress, strain, initial density, and time respectively.

It can be seen that the system of equations (1.1), (3.1) and (3.2) are hyperbolic and therefore are soluble by graphical integration along characteristics in the (x,t) plane, even when closed analytical solutions are not obtainable. This method, as it applies to plastic wave-propagation, has been described in detail in numerous publications [7,14,18,26]. Consequently, the characteristics and characteristic relations are

$$\frac{dx}{dt} = \left\{ \begin{array}{l} \pm c_0 \quad ; \quad \frac{\partial \sigma}{\partial t} < 0 \\ \pm c(\sigma, \varepsilon) \quad \frac{\partial \sigma}{\partial t} > 0 \end{array} \right\} \quad (3.3)$$

and

$$dx = 0$$

$$dv = g(\sigma, \varepsilon) dx \pm \left\{ \begin{array}{l} \frac{1}{c_0} \frac{d\sigma}{\rho} \quad \text{--(a)} \\ \frac{1}{c} \frac{d\sigma}{\rho} \quad \text{--(b)} \end{array} \right. \quad (3.4)$$

$$d\varepsilon = g(\sigma, \varepsilon) dt + \left\{ \begin{array}{l} \frac{1}{E} d\sigma \quad \text{--(a)} \\ f d\sigma \quad \text{--(b)} \end{array} \right.$$

where

$$c(\sigma, \varepsilon) = \sqrt{\frac{1}{\rho f(\sigma, \varepsilon)}} \quad (3.5)$$

and

$$c_0 = \sqrt{\frac{E}{\rho}}$$

The solution of the problem of wave-propagation is complete when the network of characteristics is determined in the (x,t) plane; and when the field variables σ , ϵ and v have been determined throughout the plane.

Because of the strain-rate effect, a loading characteristic cannot be a locus of constant state, hence the characteristics in the loading region are curved. In a numerical computation the curves must, of course, be replaced by broken lines.

If unloading takes place, an unloading wave similar to that studied by Rakhmatulin [24] must be propagated. This is an acceleration wave, i.e., on it the field variables σ , ϵ , v are continuous; but their first derivatives with respect to x and t are not; in particular

$$\frac{\partial \sigma}{\partial t} \begin{cases} > 0 & \text{ahead of the wave} \\ < 0 & \text{behind the wave} \end{cases}$$

A point (x,t) through which the locus of the unloading wave passes lies on both a loading and an unloading characteristic of the same sign; the state at (x,t) is determined along the loading characteristics, and an additional equation connects it with a neighboring point on the unloading characteristic, where the state is likewise determined. In general a trial-and-error procedure is necessary to construct the unloading curve; and the aforementioned additional equation serves to determine whether or not an assumed point lies on the curve; this is as long as the slope satisfies

$$c(\sigma, \epsilon) \leq \left| \frac{dx}{dt} \right| \leq c_0 \quad (3.6)$$

where $\sigma = \sigma(x,t)$; $\epsilon = \epsilon(x,t)$. Otherwise the unloading curve is not the locus of the acceleration wave, but simply of $\frac{\partial \sigma}{\partial t} = 0$.

In constant-velocity impact, if V_0 , the magnitude of the impact velocity, is greater than $\sigma_s/\rho c_0$ where σ_s is the static yield stress, then the initial development of the solution is that of the KTR* theory: characteristics fan out from the origin with initial slopes $c(\sigma, \epsilon)$ corresponding to states (σ, ϵ, v) , where

$$\sigma = h_d(\epsilon), \text{ the dynamic stress-strain relation} \quad (3.7)$$

$$v = \int_0^{\epsilon} c(\sigma, \epsilon) d\epsilon \quad (3.8)$$

The stress along the characteristics relaxes and they become curved. Furthermore, stress relaxation begins immediately at the impact end, so that the unloading-wave locus goes out from the origin, coinciding initially with the steepest loading characteristic.

* Strain-rate independent theory due to Kármán [30], Taylor [28], and Rakhmatulin [24].

4. Wave-Propagation in a Finite Bar:

In this section, we shall consider the propagation of plastic waves in a finite bar of length ℓ , with a fixed end at $x = \ell$. We shall assume that the magnitude, V_0 , of a sudden, constant velocity applied at $t = 0$; $x = 0$ is large enough to send plastic waves down the bar. The first quadrant of the (x,t) plane may be divided into the following regions.

Region I: $c_0 t < x < \ell$. (See Fig. 1)

Here $\sigma = \epsilon = v = 0$.

Region II: $F(t) < x < c_0 t < \ell$, where $x = F(t)$ is the locus of unloading wave; here $\sigma > \sigma_s$ and $\frac{\partial \sigma}{\partial t} > 0$, so that the characteristic slopes are $\pm c(\sigma, \epsilon)$. Finally as a result of stress relaxation at the impact end, there is an unloading region.

Region III: $0 < x < F(t)$: here $\frac{\partial \sigma}{\partial t} < 0$, so the characteristic slopes are $\pm c_0$.

It should be noted that the stress relaxation at the impact end begins immediately; so that $F(0) = 0$; furthermore it has been shown [16] that

$$c(\sigma, \epsilon) \leq |F'(t)| \leq c_0 \quad (4.1)$$

The end of the bar at $x = \ell$ is presumed to be fixed in such a way that the particle velocity, v , at that end must always be zero. Under these conditions, the particle velocities associated with a wave drop suddenly to zero at $x = \ell$ when the oncoming wave strikes this point. This shock jump in v results in shocks in stress and strain that induce new waves to travel back up the bar.

If the magnitude V_0 of the impact velocity is high enough, i.e., if

$V_0 > \sigma_d / \rho c_0$ where σ_d is the dynamic elastic limit, then the line $x = c_0 t$ is the locus of the stress discontinuity, which is initially σ_d , but which relaxes (as in the SM** theory) according to

$$x = c_0 t = \frac{2}{\rho c_0} \int_{\sigma}^{\sigma_d} \frac{d\tau}{g(\tau, \tau/E)} \quad (4.2)$$

Furthermore, when this wave reflects from the fixed end of a bar, the stress initially jumps. Because each plastic wave travels at a speed corresponding to the strain, the would-be shock is disseminated at different speeds back into the body. Therefore the shock conditions cannot be applied at $x = \ell$. Instead, the conditions along the characteristics will be used.

Region IV: $F(t) < x < F^*(t)$ where $x = F^*(t)$ is the locus of the unloading wave with $F^*\left(\frac{\ell}{c_0}\right) = \ell$ and

$$c(\sigma, \epsilon) \leq |F^*(t)| \leq c_0 \quad (4.3)$$

Here $\sigma < \sigma_s$; $\frac{\partial \sigma}{\partial t} > 0$; so that characteristic slopes are given by $c(\sigma, \epsilon)$. Finally as a result of stress relaxation at the point $(\ell, \frac{\ell}{c_0})$, there is an unloading region.

Region V: $F^*(t) < x < \ell$: here $\frac{\partial \sigma}{\partial t} < 0$; the characteristic slopes are again $\pm c_0$. The stress relaxation begins immediately at the fixed end of the bar so that $F^*\left(\frac{\ell}{c_0}\right) = \ell$.

** Viscoplastic theory of Sokolovsky [27] and Malvern [21].

5. Effect of Absorption Distance (Fig. 2)

On the basis of the preceding observations, it can be said that the distance x_a , at which the unloading wave $x = F(t)$ is absorbed, is a critical quantity for describing the significance of the strain-rate on plastic-wave-propagation; if this distance is short, then the strain-rate effect is insignificant and vice-versa. For a bar of finite length l , a particularly telling comparison would be that of x_a with the distance x_i , at which the unloading wave $x = F(t)$ intersects the reflected plastic wave. If $x_a < x_i$ the unloading wave $x = F(t)$ is absorbed before intersection, so that the further development of the wave pattern is in accordance with the "rate-independent theory", while if $x_a > x_i$, intersection takes place so that the further development is in accordance with the "viscoplastic theory". The limiting case is therefore $x_a = x_i$; in which case the development is in accordance with the "plastic-viscoplastic theory".

On the basis of the observations of Lubliner [20] for the case of an extremely simple model, and the preceding observations, it may be said that the case of $x_a > x_i$, i.e., the unloading wave $x = F(t)$ proceeds further without getting absorbed, may come about as a result of one or more of the following circumstances:

- (i) weak impact
- (ii) long bar
- (iii) short relaxation time

Then the strain-rate effect is highly significant, and, presumably, the viscoplastic theory gives a good approximation.

The converse conditions will, of course, apply if $x_a < x_i$, i.e., the

unloading wave $x = F(t)$ is absorbed before intersection. Then the strain-rate effect is insignificant and, presumably, the theory of Karman [30], Taylor [28], and Rakhmatulin [24] can give a good approximation. If, lastly, x_a is nearly equal to x_i , then, in order to obtain results which will reasonably well represent the physical situation, the plastic-viscoplastic theory of Lubliner [19] must be resorted to.

6. Computational Procedure

Since the solution in closed analytic form are seldom known for quasi-linear systems, some other method of solution must be found. To resolve this problem, we now turn to finite difference methods which may be used in many different ways to obtain numerical solutions to such problems. Existence, uniqueness and stability of the solution of the initial value problem for the hyperbolic system of 'n' quasi-linear first-order partial differential equations have been established by various authors [7,8].

It is the direct replacement of the derivative along the characteristics that forms the basis of the finite difference method. Thus we are now led to the following procedure for computing the solution of the initial value problem for equation (3.4).

Let us examine the representative points in the (x,t) net illustrated in Figure 3.. Initially, only the conditions along α_0 are known. This characteristic has a slope of c_0 . The solution for the characteristics and the field variables can then be made by approximation from time t to time $t + \Delta t$. For example, we shall sketch the procedure for finding the values of σ , ϵ and v and therefore the slopes of the α and β characteristics along the line CD , once the variables on the line AB are known. We can use these slopes to draw straight-line approximations to the characteristics throughout the region $ABCD$. Through each of the points P_0, P_1, \dots, P_n on CD , the characteristics are drawn by means of the slopes along AB . For determining the field variables along CD ; from the known values along AB , the following relations, derived from equation (3.4b) will be used:

$$\begin{aligned}
\varepsilon_T - \varepsilon_Q - f_Q(\sigma_T - \sigma_Q) &= g_Q(t_T - t_Q) \\
(v_T - v_S) + \frac{1}{\rho c_S}(\sigma_T - \sigma_S) &= -g_S c_S(t_T - t_S) \\
-(v_T - v_R) + \frac{1}{\rho c_R}(\sigma_T - \sigma_R) &= -g_R c_R(t_T - t_R)
\end{aligned} \tag{6.1}$$

The computed values of σ , ε and v along AB, together with equations (6.1) enable us to find the values of σ , ε and v at P_0, P_1, \dots, P_n . By linear interpolation, the values of σ , ε and v along CD can then be found. Successive applications of the scheme will enable the solution to be advanced further in time.

7. General Solution

We shall now be concerned with the construction of general solution to the problem for the following initial and boundary conditions.

Problem A: Semi-infinite bar:

Let us consider now the case where the velocity applied to the end of the bar is first monotone increasing from zero and then decreasing (Fig. [4]). The boundary and initial conditions are:

$$x = 0, \left\{ \begin{array}{l} 0 < t < T : v = 4V_0 t(T - t) \\ T < t : v = 0 \end{array} \right\} \quad (7.1)$$

$$x \rightarrow \infty : v = \sigma = \varepsilon = 0$$

$$t = 0 ; x > 0 : \sigma = \varepsilon = v = 0 \quad (7.2)$$

The image of the solution in the (x,t) plane will be assumed to be such as is shown in Fig. [4].

The Region I is a region of : $\sigma = \varepsilon = v = 0$. The Region II is a region of elastic strain with Riemann waves propagating in it. If the velocity acting on the end of the bar reaches the yield value $v_y = (\sigma_s / \rho c_0)$, where σ_s is the yield stress, a plastic wave starts propagating. The solution in the entire Region III proceeds on the basis of the relations (6.1) along the characteristics. If the stress developed on the end of the bar reaches a maximum value, i.e., when $\frac{\partial \sigma}{\partial t}$ at $x = 0$, changes sign, an unloading wave starts propagating. The determination of this unloading wave $x = F(t)$ will be performed simultaneously with the solution in the entire Region IV, on the basis of the relations (3.4) on the linear characteristics and the boundary condition first of (7.1). For the unloading wave $x = F(t)$, the following condition should be satisfied.

$$c(\sigma, \varepsilon) \leq \left| \frac{dx}{dt} \right| \leq c_0$$

Thus the problem is solved in a complete manner.

Problem B: Finite bar:

We shall now be concerned with the construction of general solution of the problem of wave reflection by a rigid wall, for a constant velocity impact case. The boundary and initial conditions are:

$$\begin{aligned} x = 0 ; t > 0 : v &= V_0 \text{ (constant)} \\ x = \ell : t > 0 : v &= 0 \end{aligned} \quad (7.3)$$

$$t = 0 ; 0 < x \leq \ell : v = \sigma = \varepsilon = 0 \quad (7.4)$$

We shall consider the solution in terms of the characteristic net in the (x, t) plane and for convenience we replace the time co-ordinate by $\tau = c_0 t / \ell$ and x by $\xi = x / \ell$, where ℓ is the length of the bar. The linear characteristics and the characteristic relations in the unloaded region are then

$$\begin{aligned} \frac{d\xi}{d\tau} &= \pm 1 \\ \pm dv + \frac{1}{\rho c_0} d\sigma + g c_0 \frac{\ell}{c_0} d\tau &= 0 \\ d\varepsilon - \frac{1}{E} d\sigma - g \frac{\ell}{c_0} d\tau &= 0 \end{aligned} \quad (7.5)$$

and in the loading region

$$\begin{aligned} \frac{d\xi}{d\tau} &= \pm c' \\ \pm dv + \frac{1}{\rho c} d\sigma + g c \frac{\ell}{c_0} d\tau &= 0 \\ d\varepsilon - f d\sigma - g \frac{\ell}{c_0} d\tau &= 0 \end{aligned} \quad (7.6)$$

where $c' = c/c_0$.

The boundary and initial conditions are (Fig. 5)

$$\begin{aligned} \xi = 0 ; \tau > 0 : v = V_0 \text{ (constant)} \\ \xi = 1.0 ; \tau > 0 : v = 0 \end{aligned} \quad (7.7)$$

$$\tau = 0 ; 0 < \xi \leq 1.0 : v = \sigma = \varepsilon = 0 \quad (7.8)$$

Let us describe now the method of constructing solution in each region.

Region I: $\xi > \tau$; $\sigma = \varepsilon = v = 0$ and along the leading wave front $\xi = \tau$, the field variables σ , ε and v will be calculated from the equation (4.2).

The solution in the Region II will be obtained numerically by means of the method of nets of characteristics as explained in Section 6, knowing the relations (7.6) on the characteristics. The determination of the unloading wave $\xi = \Gamma(\tau)$ will be performed simultaneously with the solution of the entire Region III. The solution in the Region III is obtained numerically by the method of nets with the relations (7.5) on the linear characteristics and the boundary condition first of (7.7). For the unloading wave $\xi = \Gamma(\tau)$; the following condition should be satisfied.

$$c'(\sigma, \varepsilon) \leq \left| \frac{d\xi}{d\tau} \right| \leq 1 ; \Gamma(0) = 0 \quad (7.9)$$

The solution in the Region IV with the simultaneous determination of the unloading wave $\xi = \Gamma^*(\tau)$, is similar to that in the Region III with the boundary condition for $\xi = 1$: $v(1, \tau) = 0$.

For the unloading wave $\xi = \Gamma^*(\tau)$, the following conditions should be satisfied.

$$c'(\sigma, \varepsilon) \leq \left| \frac{d\xi}{d\tau} \right| \leq 1 , \Gamma^*(1) = 1 \quad (7.10)$$

In the Regions III and IV, if at any section the solution of the equations for unloaded region, determines a stress equal to the previous maximum stress to which the section has been subjected, plastic flow can occur again there; and a new region in which visco-plastic wave equations must be solved is initiated. The determination of the boundaries of such a region is as discussed by Lee [16] and Clifton and Bodner [6].

8. Numerical Examples

Let us consider some numerical examples illustrating the theoretical solutions of the previous section. The manner of determining the functions $f(\sigma, \epsilon)$ and $g(\sigma, \epsilon)$, describing the mechanical behaviour of the material, has been given in Section 2. Here in this section, the actual determination of the functions $f(\sigma, \epsilon)$ and $g(\sigma, \epsilon)$ is done on the basis of the experimental results obtained by McLellan [17] and Holt et al [13].

In the numerical examples below, we shall confine ourselves to the case of strain rates of $10^{-3} \text{ sec}^{-1} < \dot{\epsilon} < 10^3 \text{ sec}^{-1}$.

The following data are assumed:

<u>Properties</u>	<u>Heat treated 4130 steel</u>	<u>Heat treated Ti - 6Al-4V</u>
Young's modulus (ksi)	29×10^3	17.5×10^3
Density (lbs/in ⁴ /sec ²)	6.75×10^{-7}	3.0×10^{-7}
Yield stress (ksi)	145	175
Yield strain (in/in)	.005	.01

For the constants K , n , A , B and C which appear in equations (2.12) and (2.16), the values obtained from the experimental curves are:

<u>Constant</u>	<u>Heat treated 4130 steel</u>	<u>Heat treated Ti - 6Al-4V</u>
K	2.405×10^{-129}	2.480×10^{-55}
n	54.6	22
A	1.453×10^{-3}	3.226×10^{-7}
B	2.225	2.867
C	-0.0645	0.01

Complete computations for each particular region of the (x, t) plane will not be given. We shall show by means of diagrams, the variability of

results at the most interesting instants only.

a) Semi-infinite bar: (parabolic velocity impact)

Figures 6 and 8 show the various regions of the (x,t) plane. There are, however, two features of the unloading-wave locus which should be especially noted. These are:

- (1) Although the velocity at the impact end continues to increase, the stress has started decreasing at the impact end, even before the maximum velocity has been reached, so that the unloading-wave locus begins as soon as the stress at the impact end started decreasing.
- (2) In the case of the titanium alloy, the time lag for the two instants at which the velocity and the stress at the impact end reach their maximum values respectively is very small when compared to the rise time of the velocity, whereas in the case of steel, the time lag for the two instants is quite considerable when compared to the rise time of the velocity. Attention is called to this point because one of the distinguishing features pointed out between the "rate dependent" theory and "rate-independent" theory has been the relaxation time effect.

Also, it has been observed that the maximum value of the stress at the impact end, as predicted by the plastic-viscoplastic theory is less than that in the case of rate independent theory. However, for both steel and titanium alloy, the difference in the maximum values predicted by both the theories is less than about 5% and 2% respectively.

b) Finite bar: (constant velocity impact)

Figs. 10 and 11 show various regions of the (x,t) plane for different values of l , the length of the bar and V_0 , the constant velocity impact.

There are, however, two distinct limiting features of the solution which should be especially noted. These are:

In the limiting case, there is every possibility of

- (1) the area of the unloading Region III ($0 < \xi < \Gamma(\tau)$) becoming the minimum possible and
- (2) the area of the loading Region II ($\Gamma(\tau) < \xi < \tau < 1$) and $\Gamma(\tau) < \xi < \Gamma^*(\tau)$ becoming the minimum possible.

When the above-mentioned two limiting features are examined as special cases of the "plastic-viscoplastic theory" proposed in this study, it becomes apparent that there are conditions under which one or other may be valid.

For example, the first limiting case may come about as a result of the initial slope of the unloading locus being the maximum, which may well be the case if the velocity of impact is much higher than that corresponding to the dynamic yield value. Also, it can be observed from Fig. 10 that the unloading Region III is becoming smaller as the absorption distance ξ_a is getting less, which may well be the case if the bar is short.

On the other hand, the possibility of area of the loading Region II becoming the minimum may come about as a result of weaker impact, as has been shown in Fig. 11 for heat treated steel.

9. Conclusions

The procedure proposed and demonstrated for determining the specific nature of an adequate mechanical behavior equation is tedious and difficult. If carried through, it will eventually furnish a quantitative criterion for the significance of the strain rate effect.

It was found that the simple rate independent theory of plastic wave propagation may provide a valid approximation under one or more of the following circumstances:

- (i) short bar
- (ii) strong impact
- (iii) long relaxation time

On the other hand, for the converse considerations, the simpler strain rate dependent theory, i.e., viscoplastic theory may well represent the physical situation.

For convenience in making comparisons, the variation of stress with distance at various instants are plotted in Figures 12, 13, 15 and 16. It might be noted that the rate dependent constitutive relation considered in this study leads to a constant or essentially constant stress region beginning at the impact end of the bar and progressing farther along the bar as time increases. Thus, the stress plateau cannot be regarded as a distinguishing feature of the rate-independent propagation theory when the velocity applied to the bar is a step function in velocity.

The most important feature of the results as seen in Figures 12 and 15, is that they show a smooth transition in behavior from that predicted by rate-independent plastic theory near the wave front to that predicted by viscoplastic theory at points sufficiently far behind the wave front.

Depending upon the parameters of the problem, the behavior may be almost entirely quasi-plastic or almost entirely quasi-viscoplastic; this is consistent with the theory presented here.

It would be of interest to see whether or not experiments using the various techniques would show similar effects.

References

- [1] Alter, B. E. K. and C. W. Curtis, "Effect of strain rate on the propagation of a plastic strain pulse along a lead bar," J.Appl.Phys., Vol. 27, No. 9, 1956, p. 1079.
- [2] Babcock, S. G., A. Kumar, and S. J. Green, "Response of materials to suddenly applied stress loads--Part 1: High strain rate properties of elevated reentry-vehicle materials at elevated temperatures," General Motors Corporation, Technical Report AFFDL-TR-G7-35, Part I, 1967.
- [3] Baker, W. E., and C. H. Yew, "Strain rate effects in the propagation of torsional plastic waves," J.Appl.Mech., Dec. 1966, p. 917.
- [4] Bodner, S. R. and R. J. Clifton, "An experimental investigation of elastic-plastic pulse propagation in aluminum rods," J.Appl.Mech., March 1967, p. 91.
- [5] Butcher, B. M. and C. H. Karnes, "Strain rate effects in metals, J.Appl.Phys., Vol. 37, No. 1, 1962, p. 402.
- [6] Clifton, R. J. and S. R. Bodner, "An analysis of longitudinal elastic-plastic pulse propagation," J.Appl.Mech., Vol. 33, Trans. ASME, Vol. 88, Series E, 1966, p. 248.
- [7] Courant, R., E. Isaacson and M. Rees, "On the solution of nonlinear hyperbolic differential equations by finite differences," Communication on Pure and Applied Math, Vol. V, 1952, p. 243.
- [8] Courant, R., and L. Peter, "On nonlinear partial differential equations with two independent variables," Communications on Pure and Applied Math, Vol. 2, No. 3, 1949, p. 255.
- [9] Cristescu, N., "Some problems of the mechanics of inextensible strings," Proceedings, International Symposium on Stress Waves in Anel. Solids, Brown University, 1963.
- [10] DeVault, G. P., "The effect of lateral inertia on the propagation of plastic strain on a cylindrical rod," J.Mech.Phys.Solids, Vol. 13, 1965, p. 55.
- [11] Habib, E. T., "High Speed Compression Tests on Copper," J.Appl.Phys., Vol. 18, 1947, p. 645.
- [12] Hauser, F. E., "Techniques for measuring stress-strain relations at high strain rates," Experimental Mechanics, August 1966, p. 1.
- [13] Holt, D. L., S. G. Babcock, S. J. Green, and C. J. Maiden, "The strain rate dependence of the flow stress in some aluminum alloys," Trans. A.S.M., Vol. 60, No. 2, 1967, p. 152.
- [14] Jeffrey, A. and T. Taniuti, "Nonlinear wave propagation with applications to physics and magneto-hydrodynamics," Academic Press, New York, 1964, p. 141.

- [15] Kolsky, H., and L. S. Douch, "Experimental studies in plastic wave propagation," *J.Mech.Phys. Solids*, Vol. 10, 1962, p. 195.
- [16] Lee, E. H., "A boundary-value problem in the theory of plastic wave propagation," *Quart.Appl.Math.*, Vol. 10, 1953, p. 335.
- [17] McLellan, D. L., "Constitutive equations for mechanical properties of structural materials," *AIAA Journal*, Vol. 5, No. 3, 1967, p. 446.
- [18] Lister, M., "The numerical solution of hyperbolic partial differential equations by the method of characteristics," *Mathematical Methods for Digital Computers*, Chapter 15, A. Ralston and H. S. Wolf, editors, John Wiley & Sons, Inc.
- [19] Lubliner, J., "A generalized theory of strain rate dependent plastic wave propagation in bars," *J.Mech.Phys.Solids*, Vol. 12, p. 59.
- [20] Lubliner, J., "The strain rate effect in plastic wave propagation," *Journal de Mécanique*, Vol. 4, No. 1, 1965, p. 111.
- [21] Malvern, L. E., "Plastic wave propagation in a bar of material exhibiting a strain rate effect," *Quart.Appl.Math.*, Vol. 8, 1951, p. 405.
- [22] Nowacki, W. K., "Propagation and reflection of a plane stress wave from a deformable support in an elastic-visco-plastic strain hardening body," *Proceedings, Vibration Problems*, 4, 5, Warsaw, 1964, p. 297.
- [23] Rajnak, S. and F. E. Hauser, "Plastic wave propagation in rods," *Symposium on the Dynamic Behavior of Materials*, ASTM Special Technical Publication, No. 336, 1962, p. 167.
- [24] Rakhmatulin, Kh. A., "The propagation of an unloading wave," in *Russian, Prikl.Mat.Meckh.*, Vol. 9, 1945, p. 91.
- [25] Ripperger, E. A., and H. Waltson, Jr., "The relationship between the constitutive equation and one-dimensional wave propagation," (*Symposium on the Mechanical Behavior of Materials Under Dynamic Loads*, San Antonio, Texas, Sept. 1967.)
- [26] Simmons, J. A., F. Hauser, and J. E. Dorn, "Mathematical theories of plastic deformation under impulsive loading," *Univ. of California publications in Engineering*, Vol. 5, No. 7, 1962, p. 177 - 230.
- [27] Sokolovsky, V. V., "The propagation of elastic, viscous plastic waves in bars," *ONR translation No. 6*, from *Prikladnaia Matematika i Mekhanika*, Vol. 12, 1948, p. 261 - 280, *Grad.Div., Appl.Math.*, Brown Univ., Feb. 1949.
- [28] Taylor, G. I., "The plastic wave in a wire extended by an impact load," *Scientific papers*, G. K. Batchelor, editor, Vol. 1, Cambridge Press, 1958, p. 467.
- [29] Ting, T. C. T., and P. S. Symonds, "Longitudinal impact on viscoplastic-linear stress-strain rate law," *J.Appl.Mech.*, June 1964, p. 199.
- [30] VonKarman, T. and P. Duwez, "The propagation of plastic deformation in solids," *J.Appl.Phys.*, Vol. 21, 1950, p. 987.

- [31] White, M. P. and L. V. Griffes, "The propagation of plasticity in uniaxial compression," J.Appl.Mech., Sept. 1948, p. 256.
- [32] Yoshida, S. and N. Nagata, "Deformation of polycrystalline aluminum at high strain rates," Trans.Japan Institute of Metals, Vol. 7, No. 4, 1966, p. 273.

List of Figures

- Fig. 1: x-t plane diagram
- Fig. 2: x-t plane diagram
- Fig. 3 Schematic diagram for numerical solution
- Fig. 4: x-t plane diagram (semi-infinite bar)
- Fig. 5: x-t plane diagram (finite bar)
- Fig. 6: x-t plane diagram for heat treated Ti-6Al-4V, room temperature
- Fig. 7: Variation of stress with x for heat treated Ti-6Al-4V, room temperature
- Fig. 8: x-t plane diagram for heat treated 4130 steel, room temperature
- Fig. 9: Variation of stress with x for heat treated 4130 steel, room temperature
- Fig. 10: x-t plane diagram for heat treated 4130 steel, room temperature
(constant velocity impact of 200 fps)
- Fig. 11: x-t plane diagram for heat treated 4130 steel, room temperature
(constant velocity impact of 120 fps)
- Fig. 12: Variation of stress with x for heat treated 4130 steel, room temperature.
- Fig. 13: Variation of stress with x for heat treated 4130 steel, room temperature
- Fig. 14: x-t plane diagram for heat treated Ti-6Al-4V, room temperature
(constant velocity impact)
- Fig. 15: Variation of stress with x for heat treated Ti-6Al-4V, room temperature
- Fig. 16: Variation of stress with x for heat treated Ti-6Al-4V, room temperature.

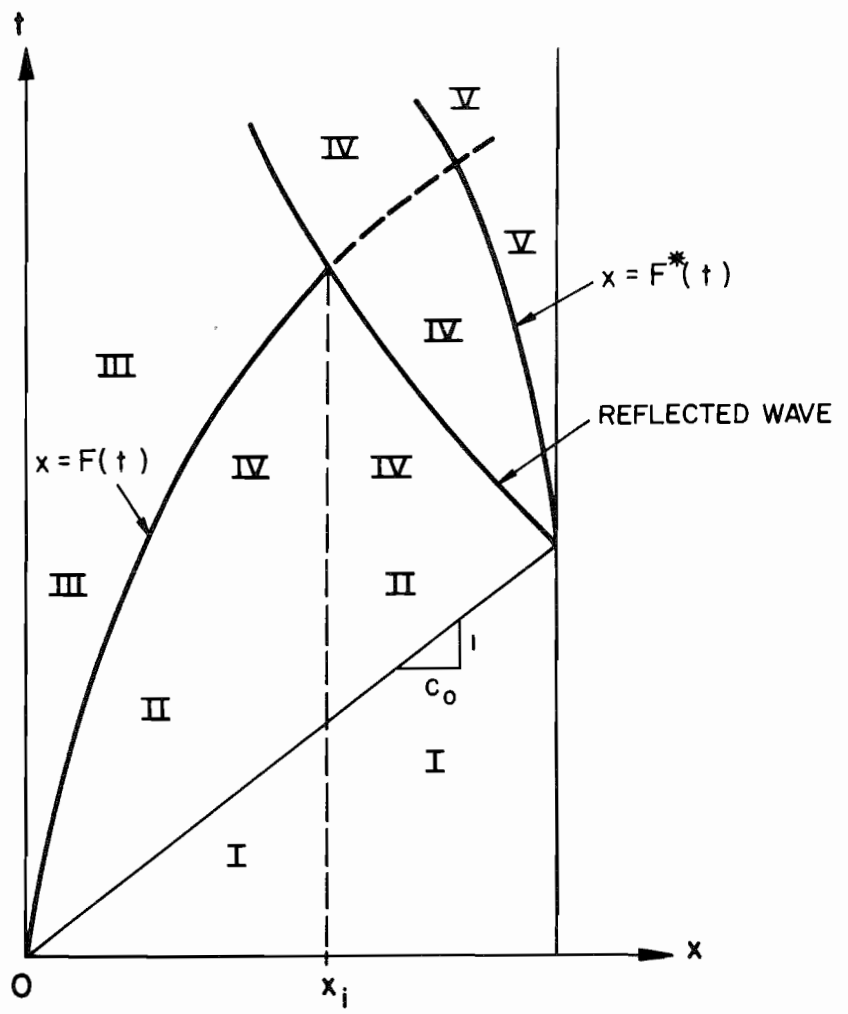


FIG. I x-t PLANE DIAGRAM

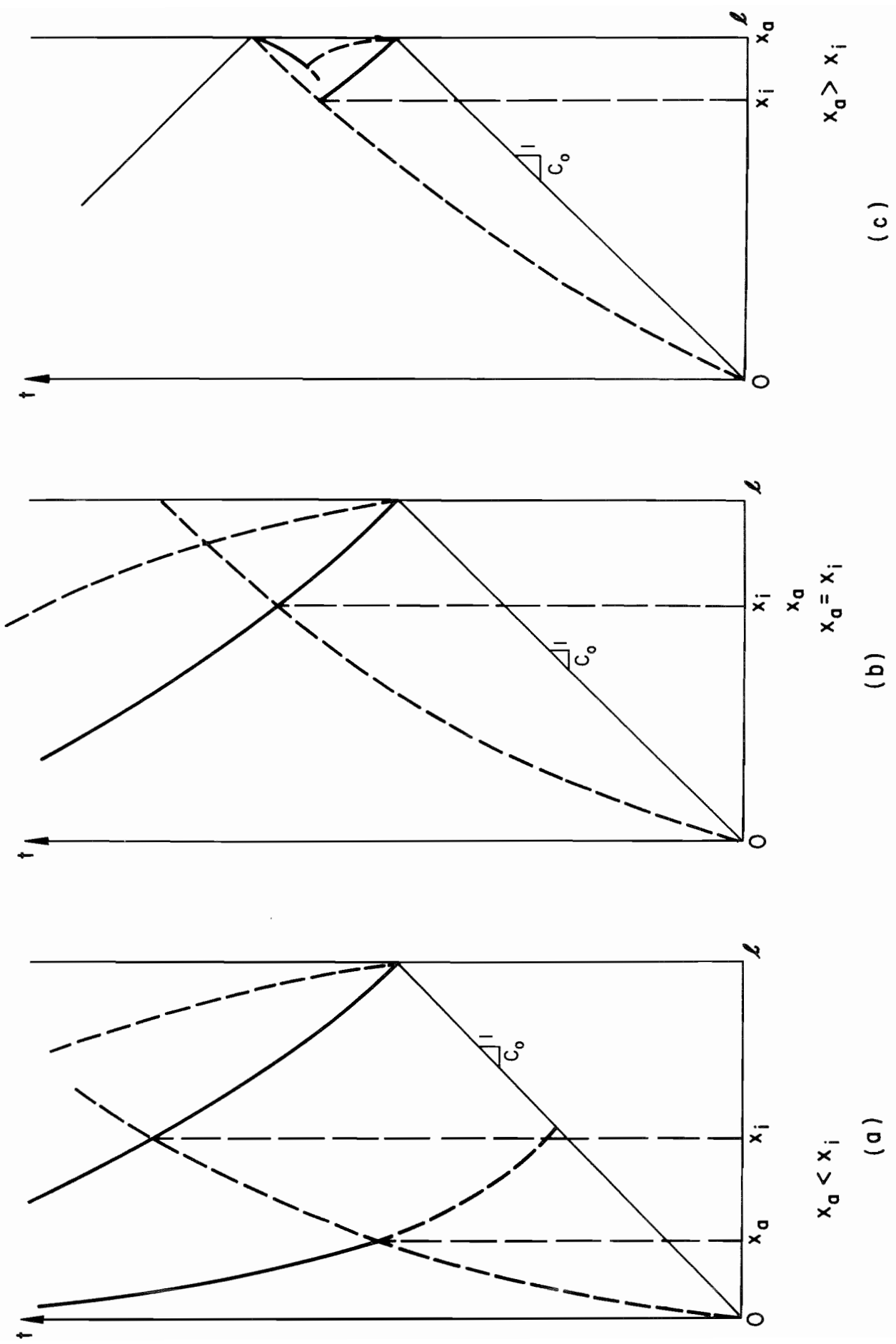
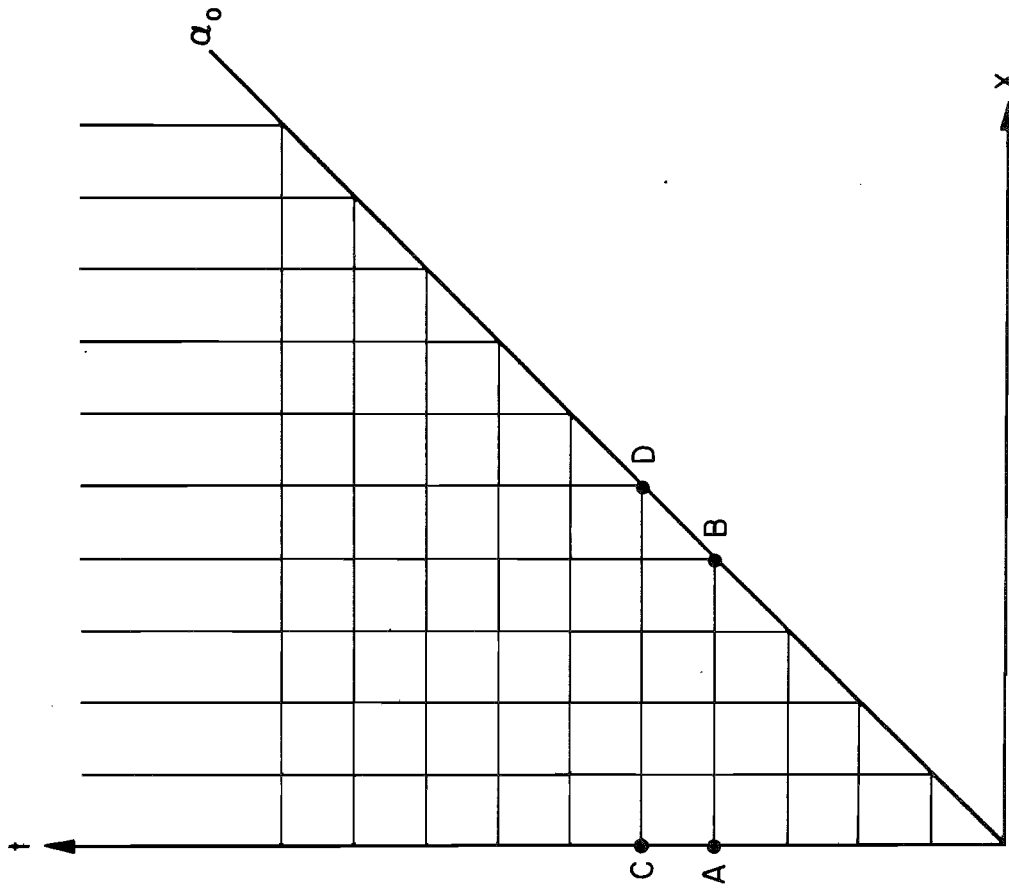
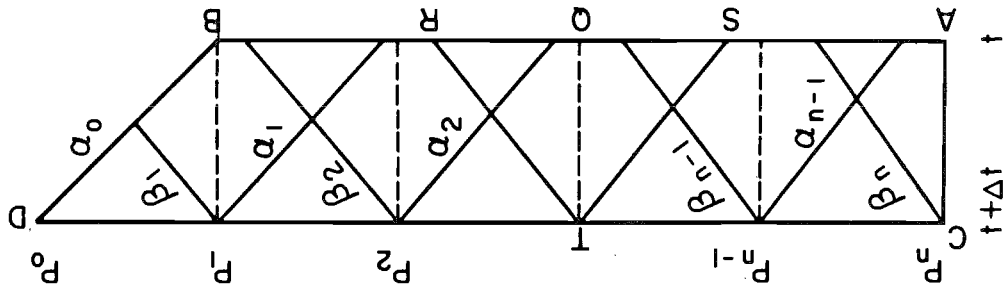


FIG. 2 x - t PLANE DIAGRAM



SCHMATIC DIAGRAM FOR NUMERICAL SOLUTION



MAGNIFIED SECTION SHOWING REGION BETWEEN AB AND CD

FIG. 3

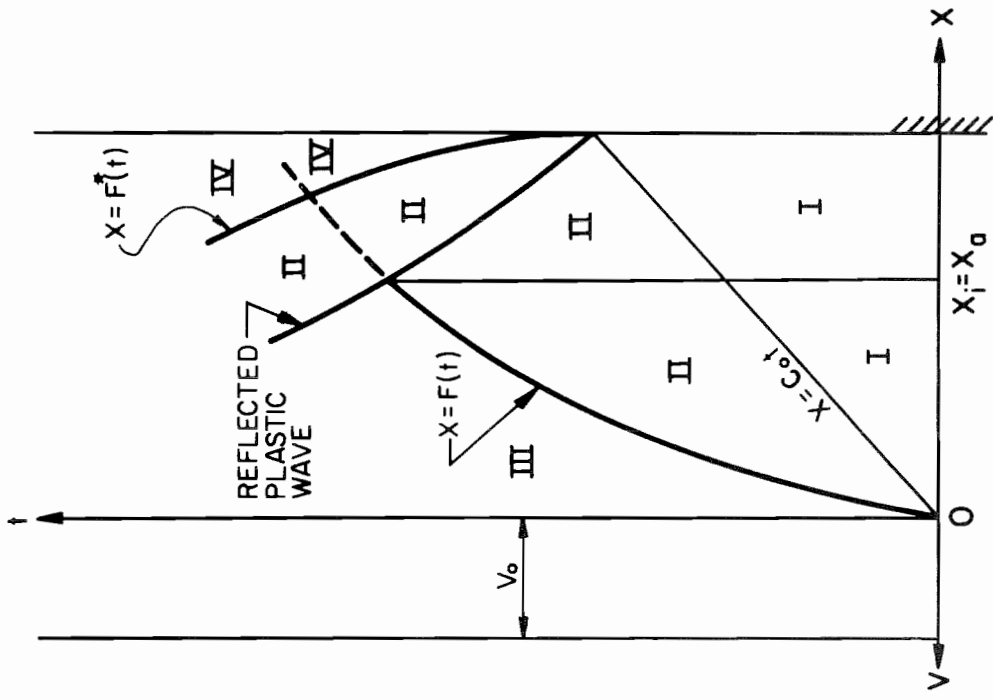


FIG. 5 x - t PLANE DIAGRAM
(FINITE BAR)

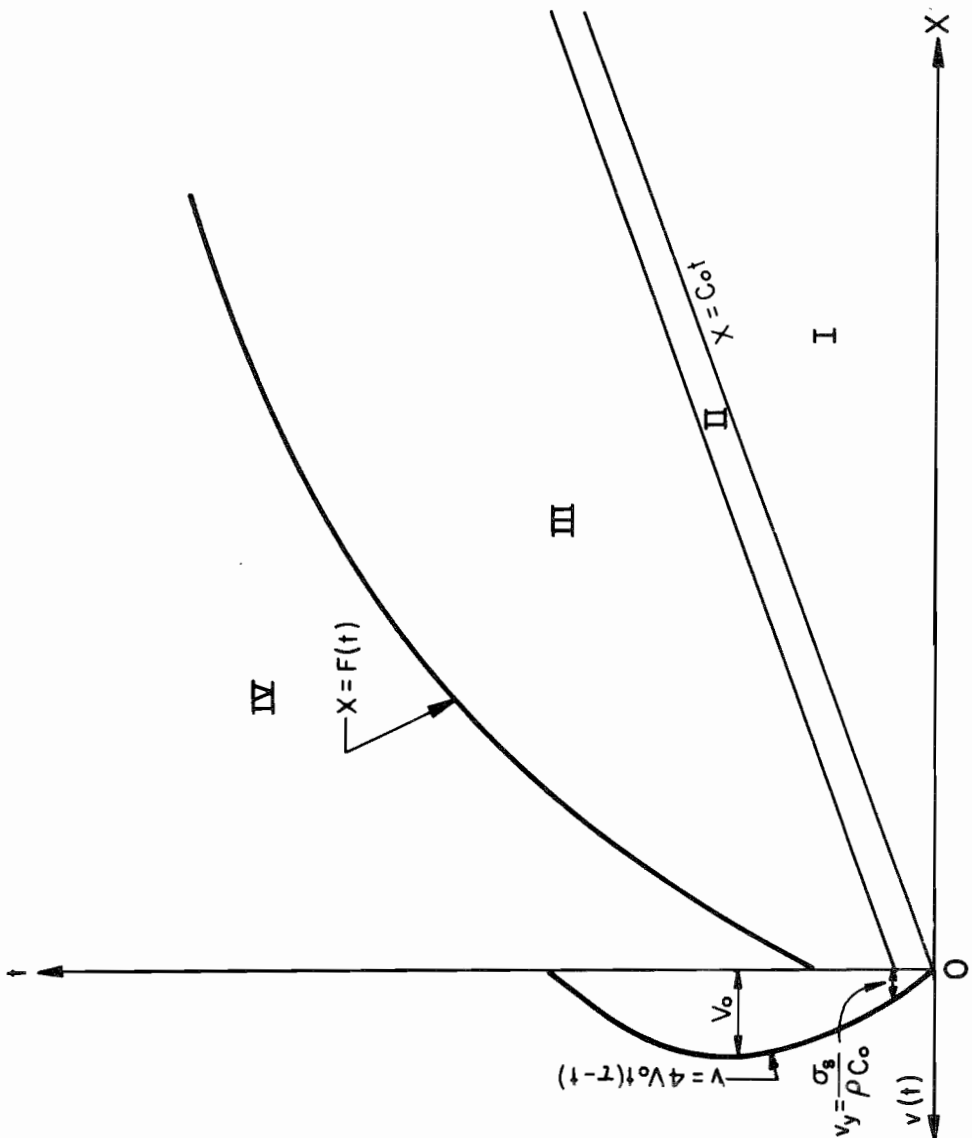


FIG. 4 x - t PLANE DIAGRAM
(SEMI - INFINITE BAR)

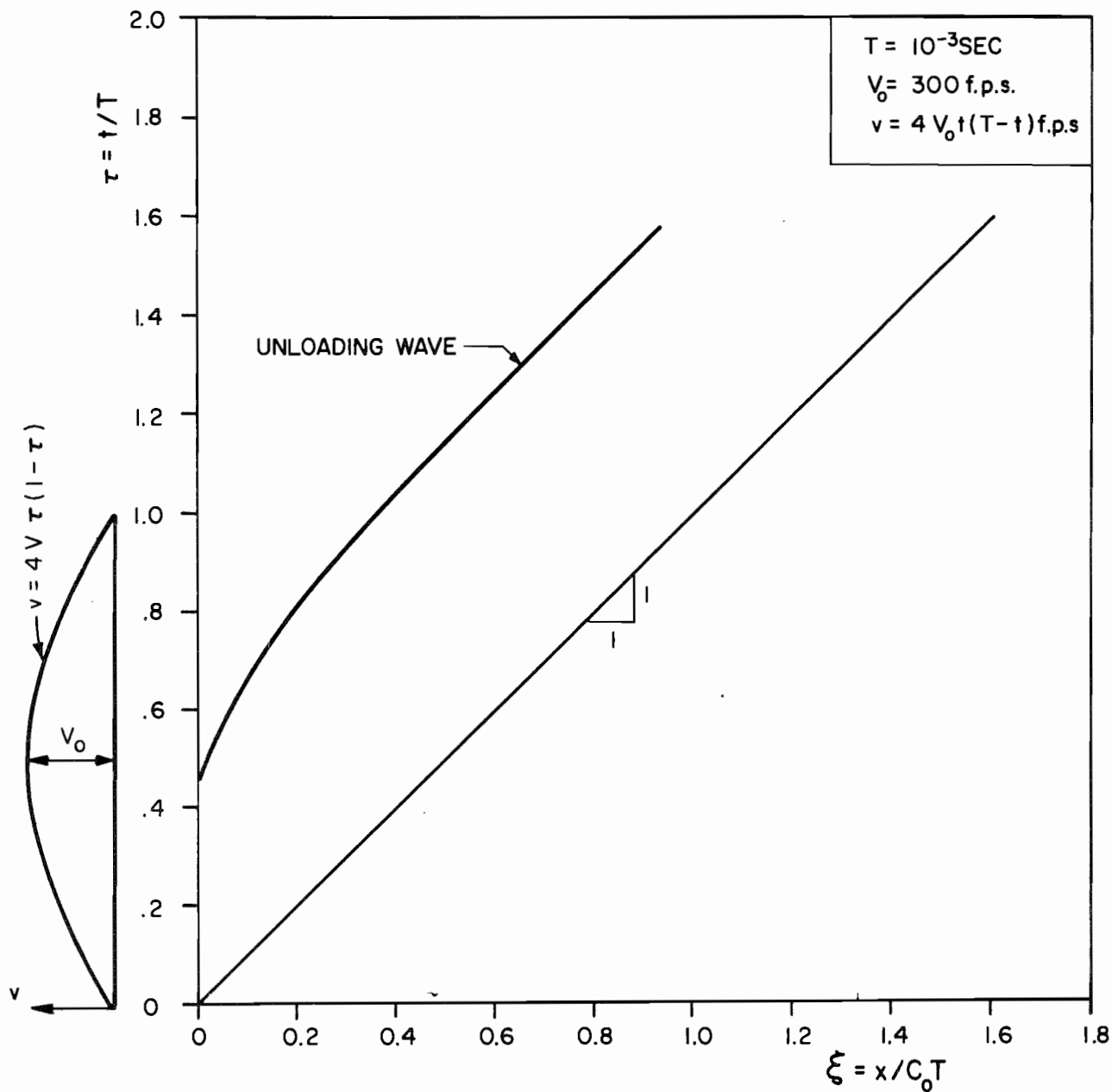


FIG. 6 $x-t$ PLANE DIAGRAM FOR HEAT TREATED Ti-6Al-4V, ROOM TEMPERATURE (PARABOLIC VELOCITY IMPACT)

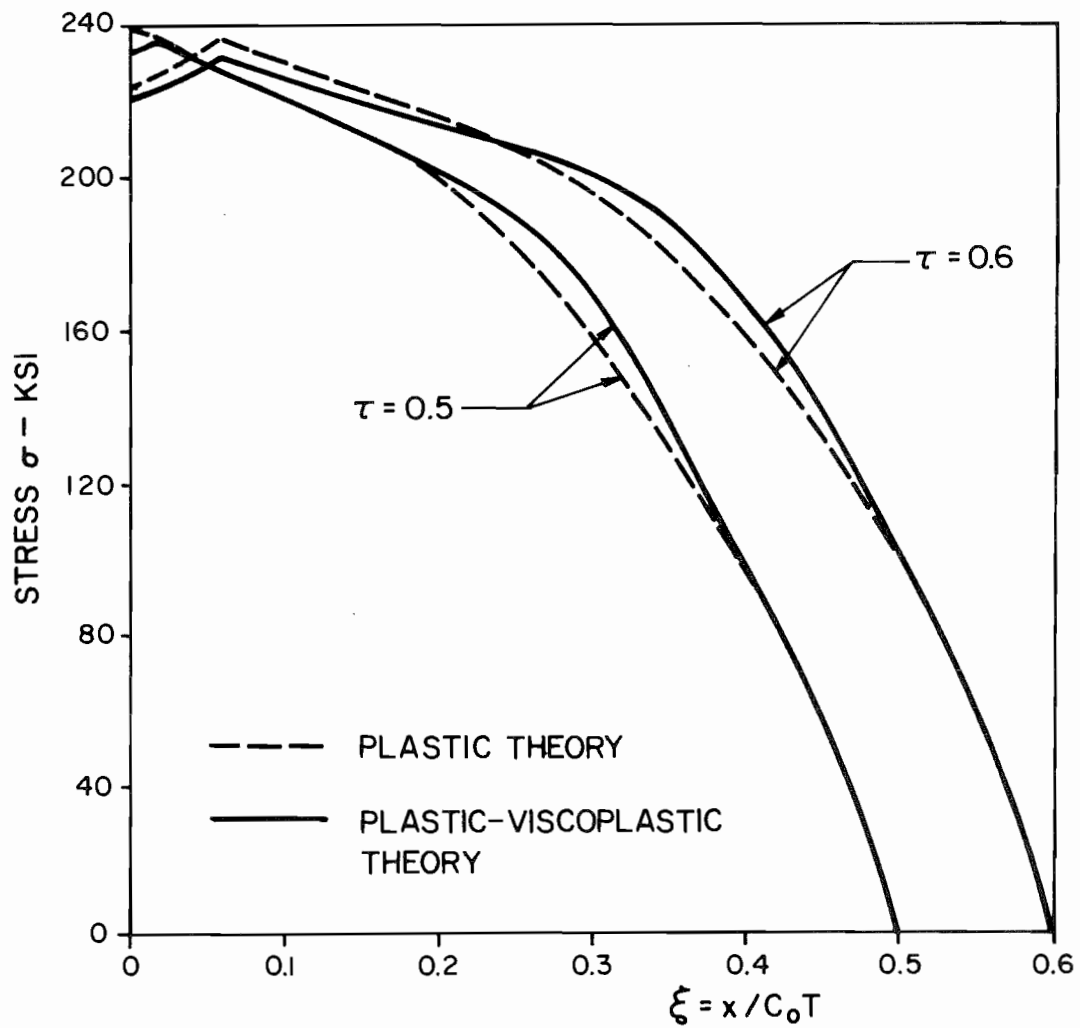


FIG. 7 VARIATION OF STRESS WITH x FOR HEAT TREATED Ti-6Al-4V, ROOM TEMPERATURE

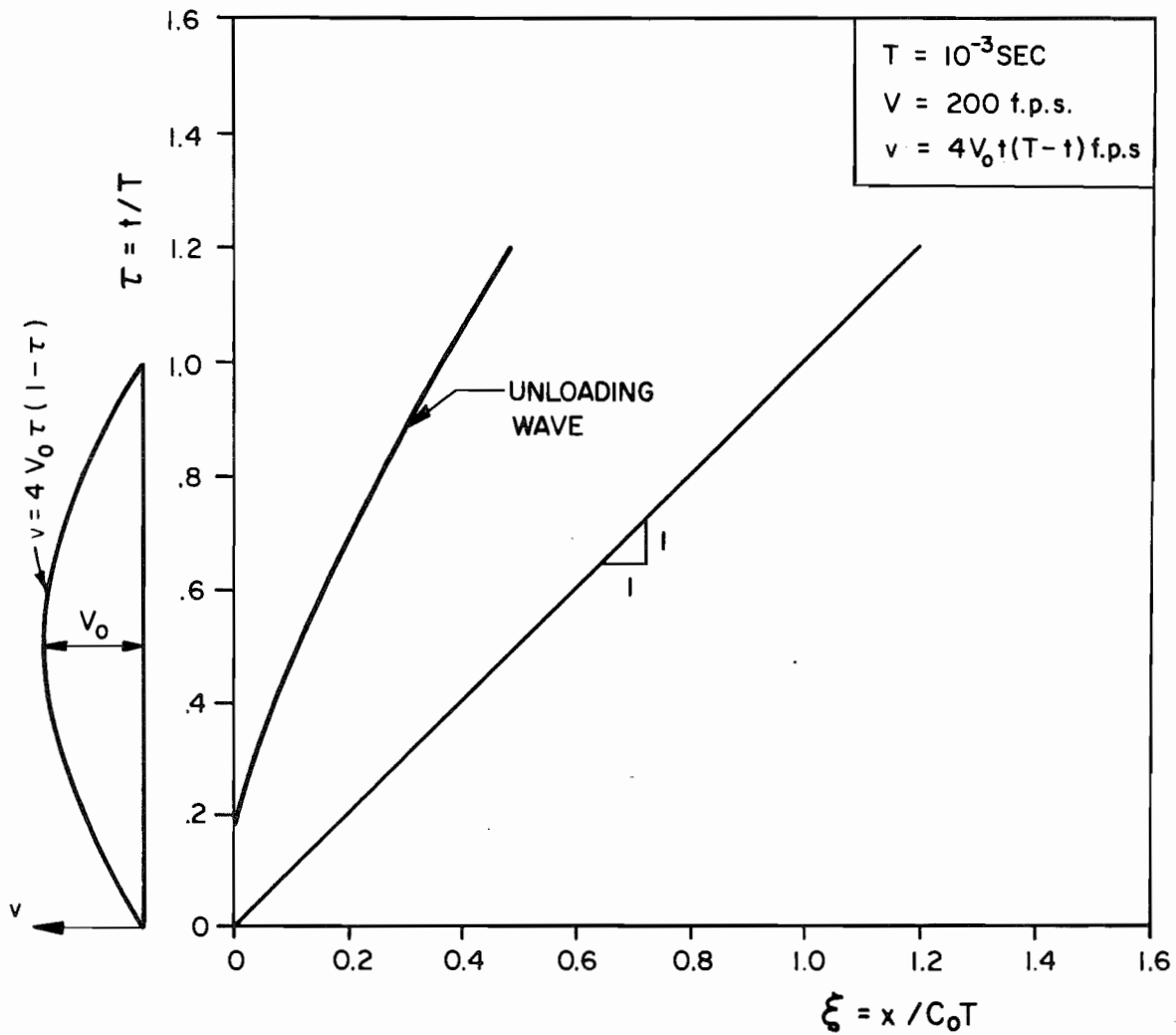


FIG. 8 $x-t$ PLANE DIAGRAM FOR HEAT TREATED 4130 STEEL, ROOM TEMPERATURE (PARABOLIC VELOCITY IMPACT)

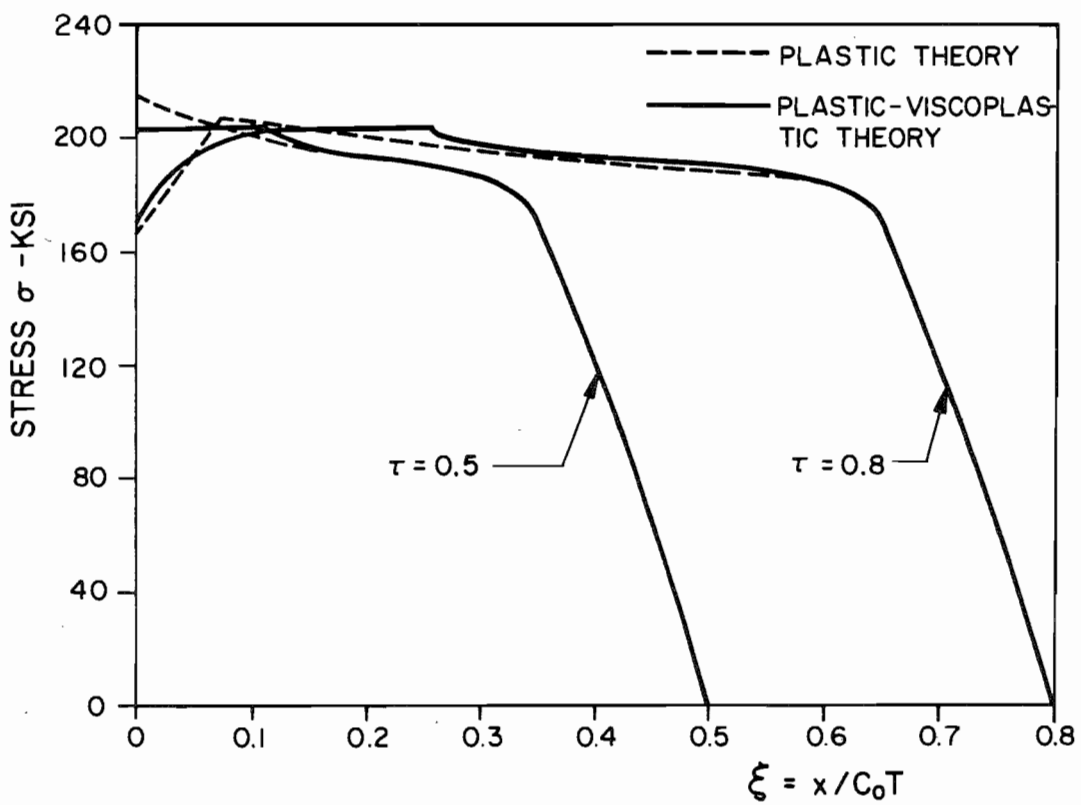


FIG.9 VARIATION OF STRESS WITH x FOR HEAT TREATED 4130 STEEL, ROOM TEMPERATURE

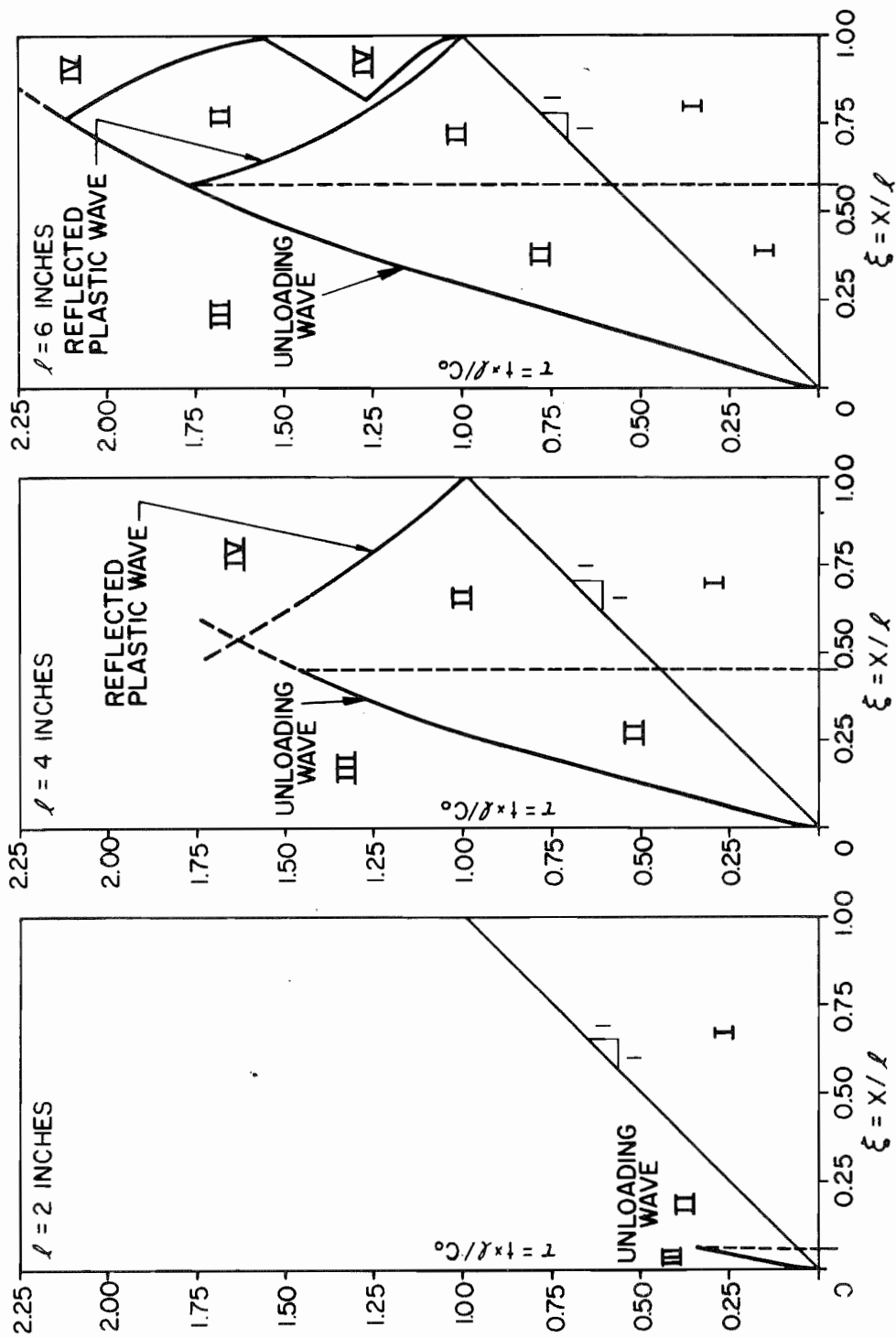


FIG. 10 x-t PLANE DIAGRAM FOR HEAT TREATED 4130 STEEL, ROOM TEMPERATURE (CONSTANT VELOCITY IMPACT OF 200 f.p.s.)

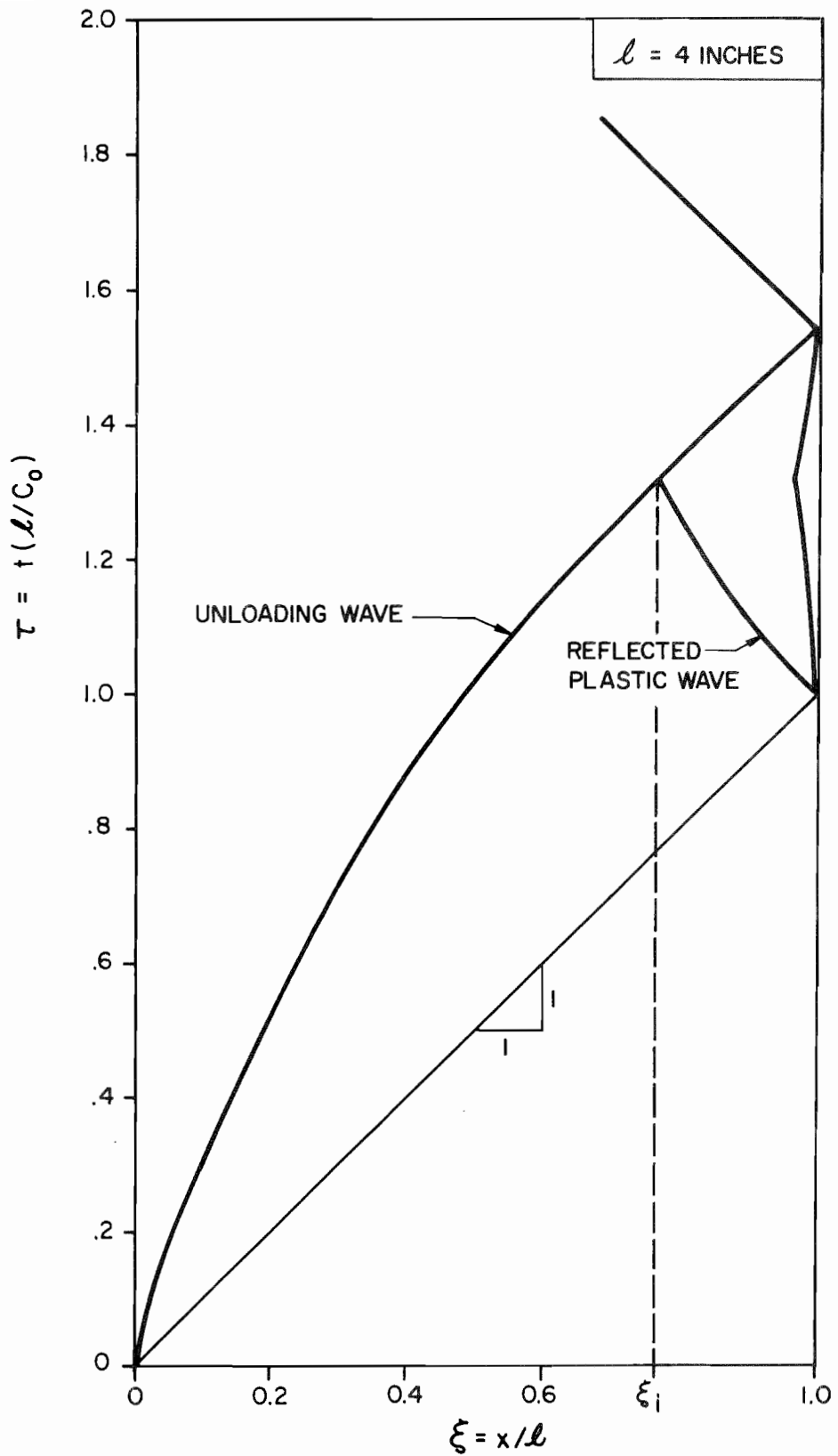


FIG. II $x-t$ PLANE DIAGRAM FOR HEAT TREATED 4130 STEEL, ROOM TEMPERATURE (CONSTANT VELOCITY IMPACT OF 120 f.p.s.)

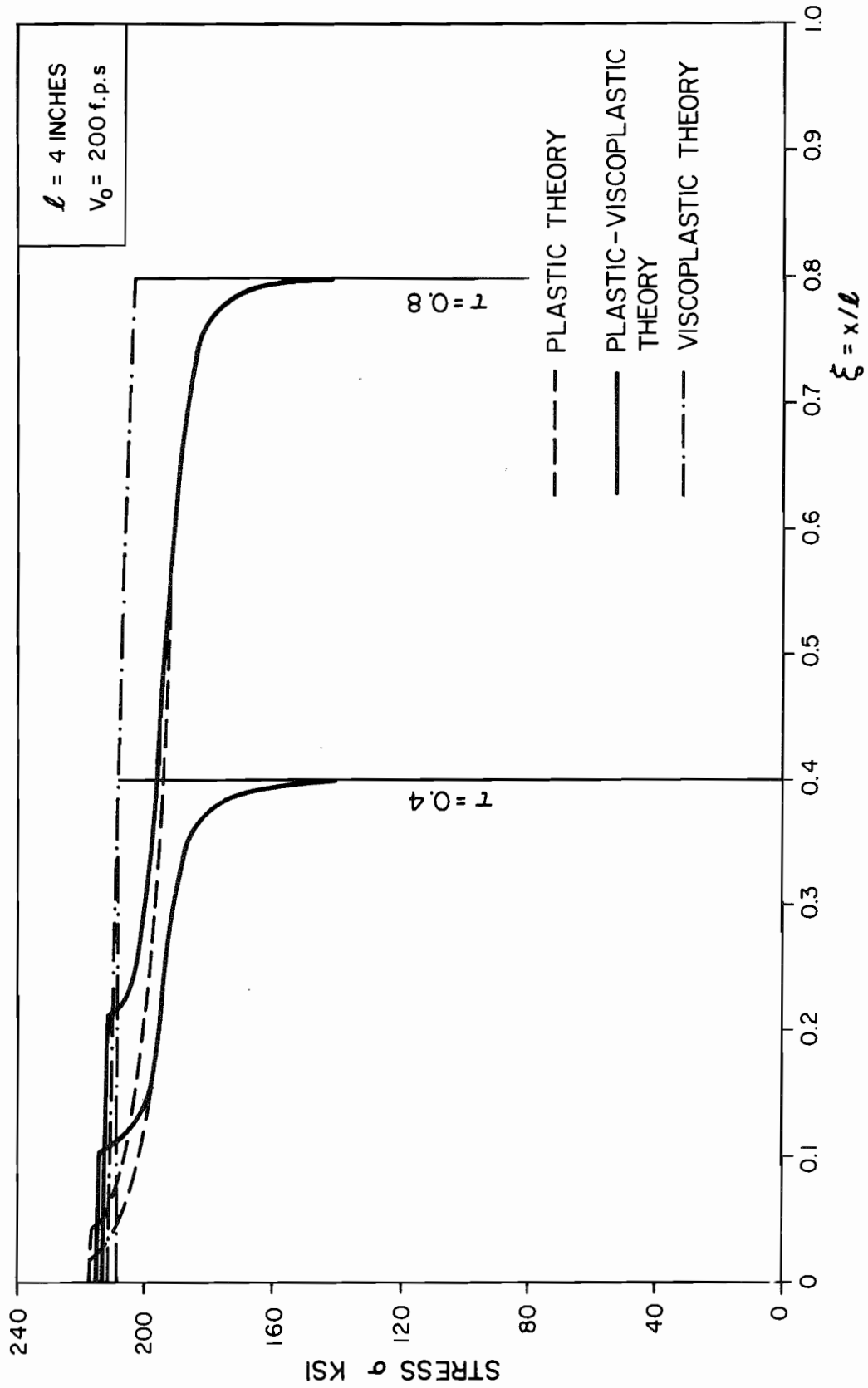


FIG. 12 VARIATION OF STRESS WITH x FOR HEAT TREATED 4130 STEEL, ROOM TEMPERATURE

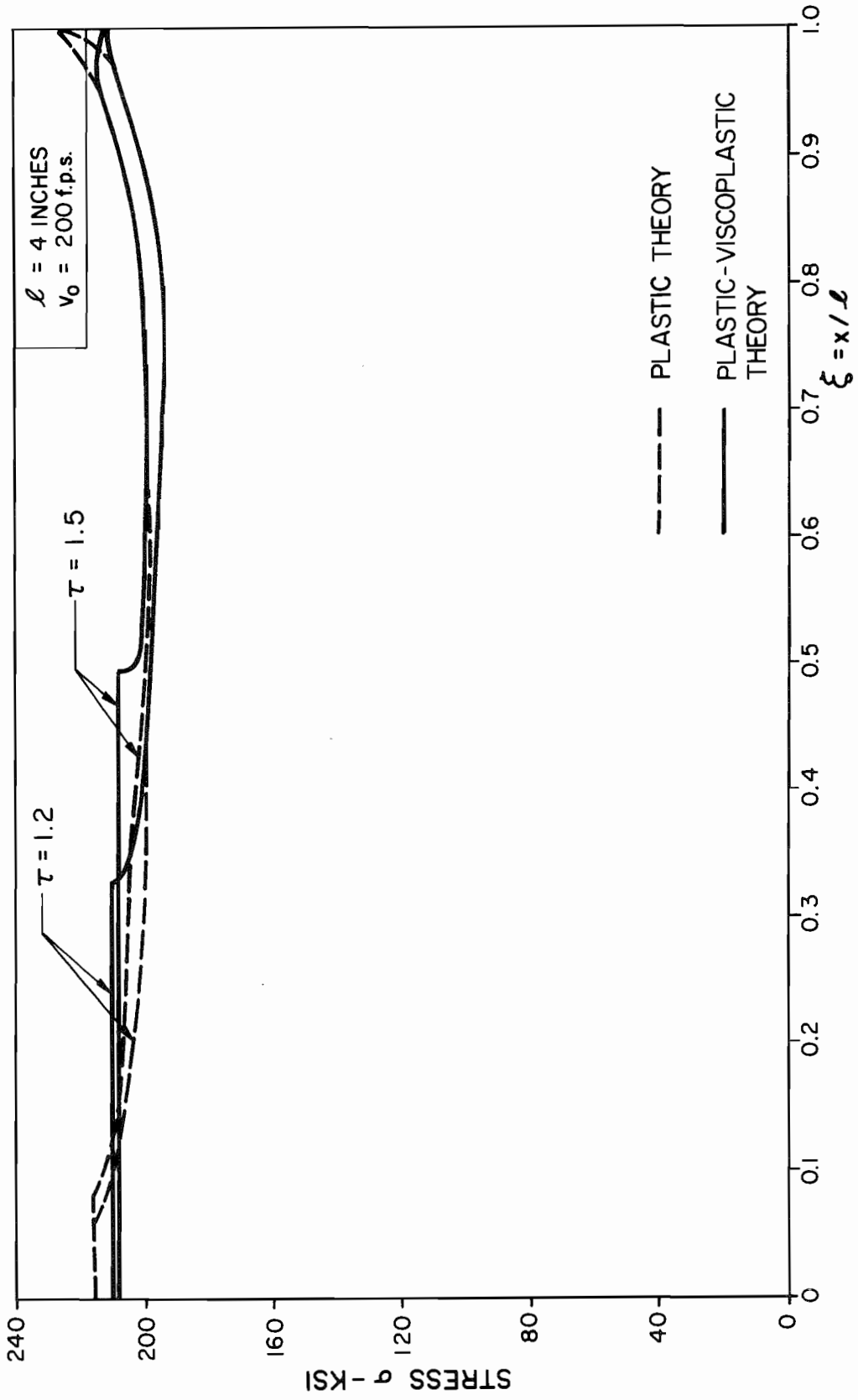


FIG. 13 VARIATION OF STRESS WITH x FOR HEAT TREATED 4130 STEEL, ROOM TEMPERATURE

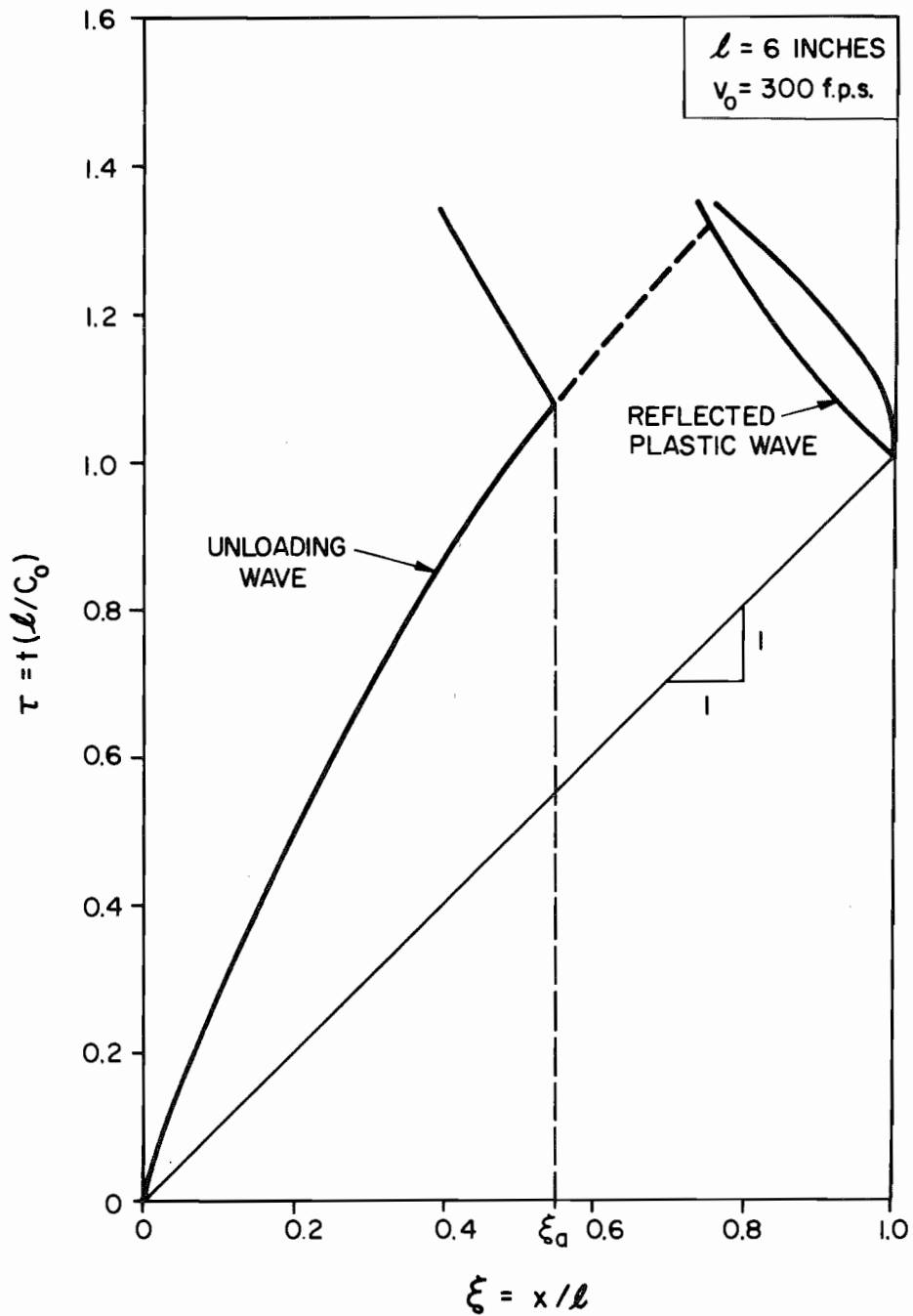


FIG.14 $x-t$ PLANE DIAGRAM FOR HEAT TREATED Ti-6Al-4V, ROOM TEMPERATURE (CONSTANT VELOCITY IMPACT)

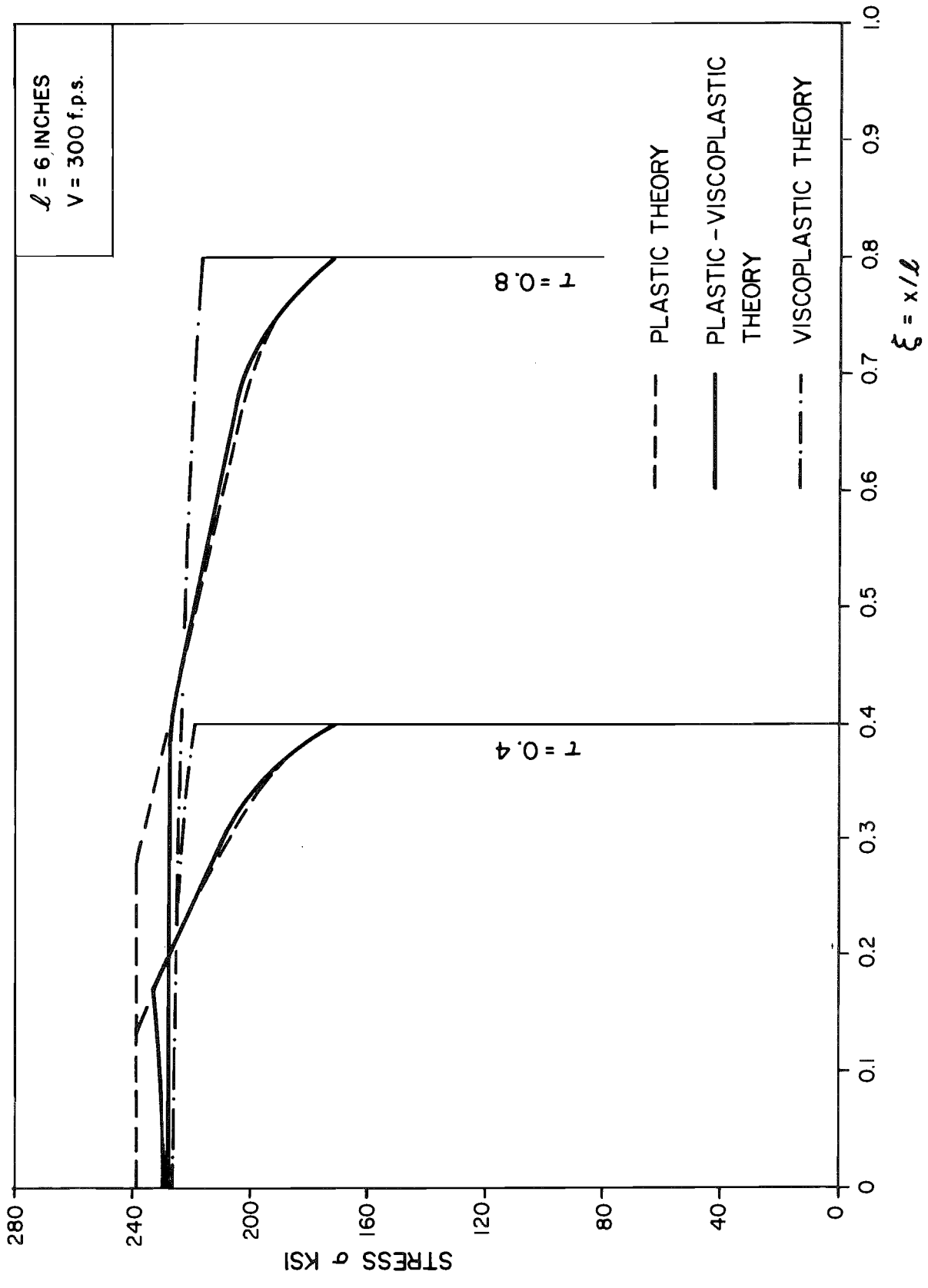


FIG.15 VARIATION OF STRESS WITH x FOR HEAT TREATED Ti-6Al-4V, ROOM TEMPERATURE

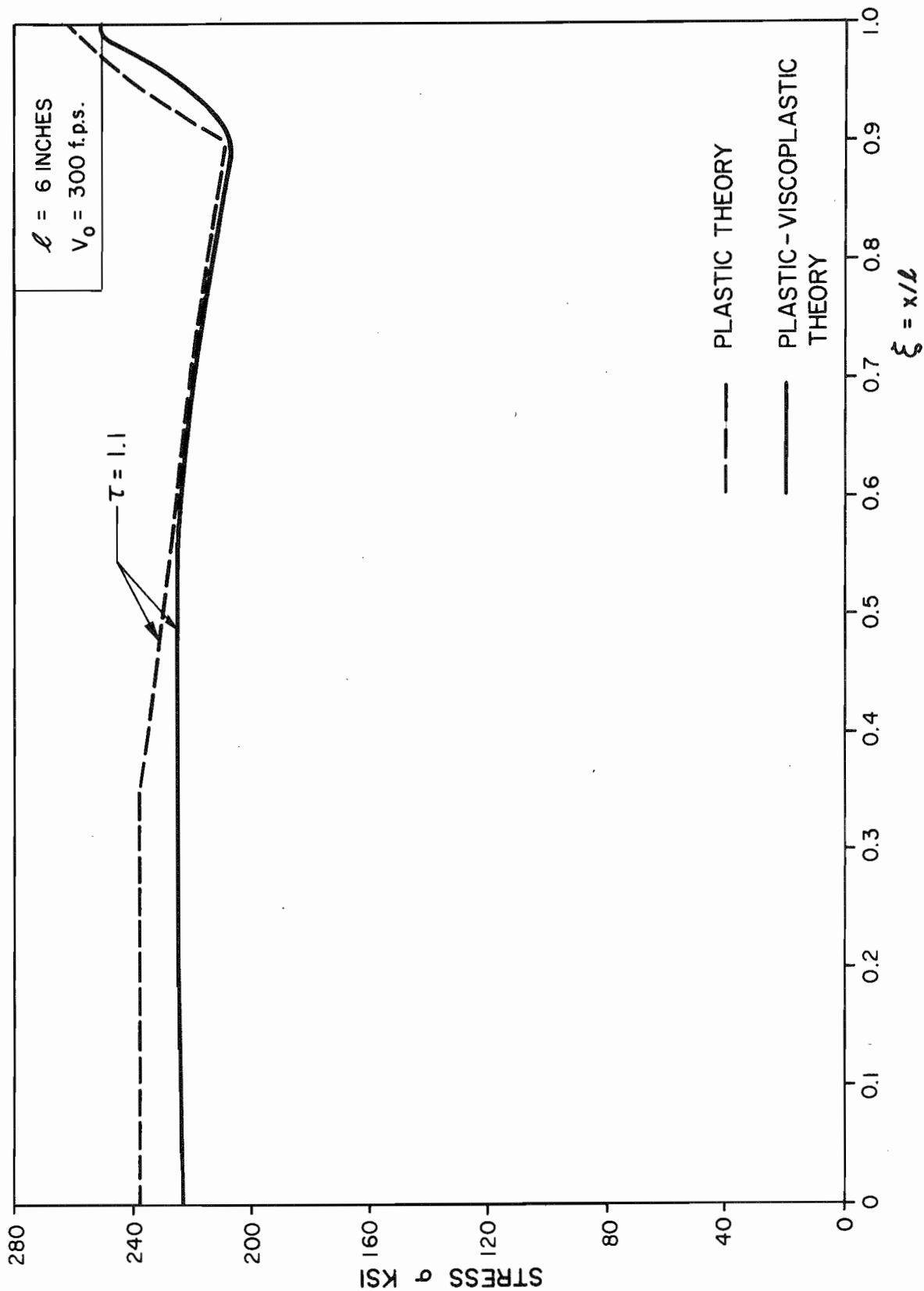


FIG.16 VARIATION OF STRESS WITH x FOR HEAT TREATED Ti-6Al-4V, ROOM TEMPERATURE